Deep Learning for Quantitative Image Analysis of Morphological Changes in Podocyte Foot Processes in Electron Micrographs of Rat Model of Passive Heymann Nephritis

Sarah R Vargas[1], Casey Ritenour[1], Cheryl Tyszkiewicz[2], Seo-Kyoung Hwang[2], Chang-Ning Liu[2], Lindsay Tomlinson[1], Stephen Berasi[3], Xueping Fan[4], Weining Lu[4], Hongying Yang[3].

[1]Global Pathology and [2]Comparative Medicine, Drug Safety R&D, Pfizer Inc., [3]Emerging Science & Innovation/Centers for Therapeutic Innovation, Pfizer Inc., [4]Nephrology Section, Department of Medicine, Boston Medical Center.

Abstract

Podocyte injury is the final common pathway of glomerular diseases which are not adequately controlled by the current standards of care and progress to end stage renal disease (ESRD) at high incident rates. Therapies that improve podocyte structure and function could be transformative for patients with podocytopathies. Two monoclonal antibodies were tested in rat model of Passive Heymann Nephritis and their effects on podocyte foot process structure were evaluated by quantitation of podocyte foot process width on TEM images of glomeruli. The deep learning artificial intelligence module of Visiopharm was explored as a solution to speed the analysis of morphological changes of mouse podocyte foot processes in Transmission Electron Microscopy(TEM) Images. Manual measurement is time consuming and constitutes the slowest step in data analysis of this study type. Deep learning algorithms reduce the time needed to manually annotate electron micrographs, but due to micrographs consisting of a single 8-bit grayscale channel, the selection criteria of images for analysis must be strict in order to reduce the need for time consuming human intelligence tasks. Changes in traditional TEM processing and imaging should emphasize thinner sections for more discrete ultrastructure visualization, consistent contrast, consideration for cell spacing and exclusion of compressed or sub-optimally fixed tissues

Background and Study Design

Normal podocyte structure consists of intercalated finger-like projections surrounding a central capillary forming the podocyte foot process (FP) with filtration slits between each digit. The capillary lumen is surrounded by the glomerular basement membrane (GBM) which is underlaid by a network of fenestrated endothelium, above the basement membrane is the site of filtration, the podocyte food processes that are attached to the membrane, between which are the slit diaphragms (Fig. 1). This is a highly dynamic process that responds to glomerular injury with foot process fusion/effacement.

When the podocytes respond to injury the slit diaphragms are largely unchanged, the spacing between them becomes larger as the foot process expands to contact a larger surface of the basement membrane. Foot process effacement is linked to compromise of the filtration barrier and accompanied by proteinuria. Improvement in podocyte foot process effacement correlates with long term clinical benefits in lupus nephritis.

Great strides have been made in reconstructing the structure of single protein particles imaged via TEM, and in the analysis of composition of inorganic materials at both the macro- and nanoscale. These types of samples tend to have a more uniform or predictable morphology than that of a cell or tissue crowded with organelles, membranes and other features with subtle variations in texture and contrast.

Image analysis of electron micrographs of biological thin sections has lagged behind that of other imaging techniques and is traditionally accomplished by time consuming manual or semi-manual annotation which is vulnerable to unintentional bias.

The main challenge that leads to difficulty in developing automated analysis algorithms is the fact that electron micrographs consist of a single greyscale channel, whereas light and fluorescent images have at least 3 color channels that can be filtered independently to tease out features. Because of their monochromatic nature, algorithms based on image texture and patch analysis tend to perform better than those that classify based on simple thresholding or intensity. Deep learning in which the computer learns useful features and representations in an image automatically is well suited for the analysis of greyscale datasets generated from CT, MRI and Electron Microscopy. Other factors that impede analysis are the same issues that plague light and fluorescence techniques: inconsistent staining, tissue fixation, sampling, sectioning and imaging conditions that lead to variations between images and samples.

The underlaying efficacy study compared monoclonal antibodies (mAbA and mAbB) against an isotype control in the Passive Heymann Nephritis (PHN) rat model.

Treatment Groups:

1. Sham(n=2)
2. mAbA 25 mg/kg (n=6)
3. mAbA 5 mg/kg (n=6)
4. mAbB 25 mg/kg (n=6)
5. Isotype Control (Anti-FX1A) (n=6)

Animals in the sham group were not dosed and these animals served as normal, healthy, age-matched controls and to compare the histopathology of kidneys with Anti-Fx1A dosed group. Anti-Fx1A was administered by IV injection (lateral tail vein) once on Day 2 to all animals in groups 2-5

mAbA (5 or 25 mg/kg) and mAbB (25 mg/kg) doses were administered by subcutaneous injection every 3 days on Days 1, 4, 7, 10, 13, 16 to animals in groups 2,3 and 4 respectively. Group 5 was injected with Isotype control IgG.

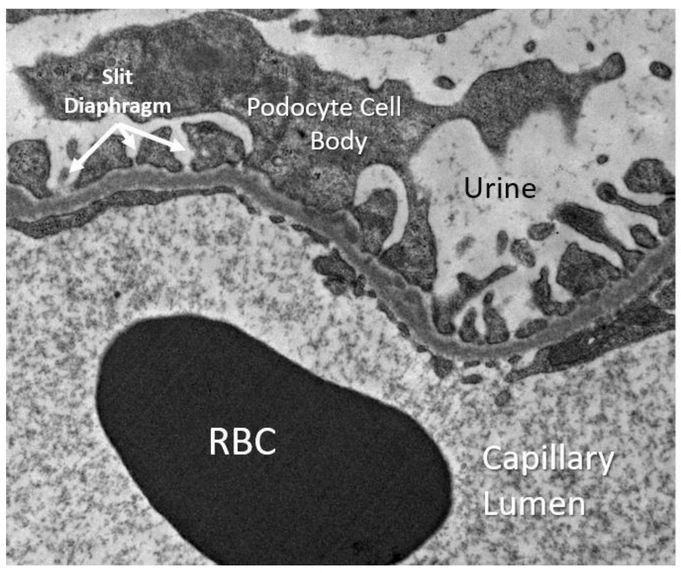

Figure 1
Electron Micrograph of Podocyte Anatomy and Ultrastructure

Methods

Processing: Samples were received in EM fixative (2.5% glutaraldehyde / 2% paraformaldehyde in 0.1M phosphate buffer), trimmed and held at 4ºC until processed.

Samples were washed 3 x 10 minutes with 0.1M buffer and then post-fixed in 1% buffered osmium for 2 hours at 25ºC. Following osmication, tissues were washed 2 X with DI water, dehydrated through a graded alcohol series, transitioned through acetone and infiltrated in a resin/acetone mixture overnight at RT. Dehydration and infiltration were carried out on a shaking platform. Samples were changed to pure resin and infiltrated 3x for at least 1 hr each prior to embedding.

Embedding: Samples were embedded and allowed to cure for at least 24 hours at 60ºC prior to sectioning.

TEM Imaging: 0.5 micron sections were mounted on glass slides and stained with toluidine blue. Blocks were then trimmed further to contain regions of interest and thin sections of 70 nm were mounted on copper grids.

Image Acquisition:

Grids were evaluated in a Hitachi H-7100 transmission electron microscope and images were captured using a BioSpirit digital CCD camera system at 5000x and 10000x magnification.

Image Selection Criteria (Fig. 2)

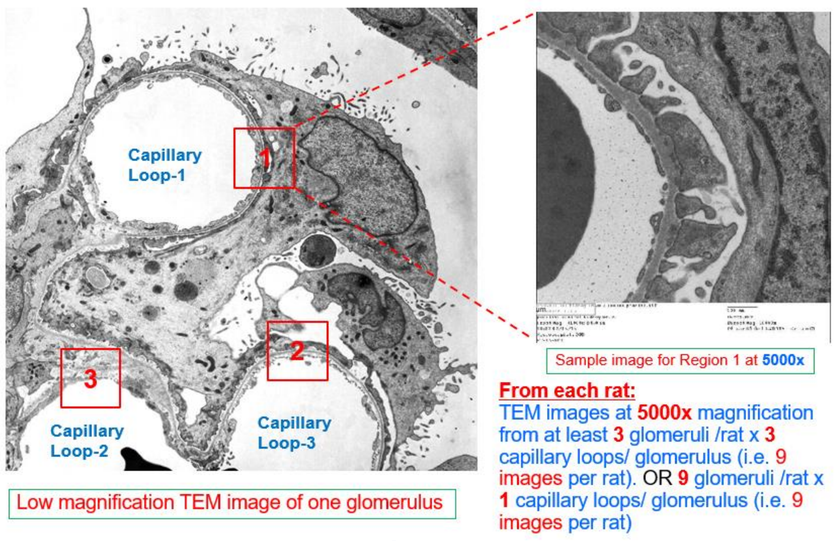

Figure 2
Image Selection Criteria

Manual Measurement

Podocyte foot process width was manually measured using ImageJ software by drawing a line parallel to the GBM from one slit diaphragm to the next.

Digital Image Analysis (DIA)

The Deep Learning module of Visiopharm was used to develop an image analysis algorithm to identify GBM, podocyte cell bodies and light areas of electron micrographs. Analysis proceeded sequentially with an initial algorithm to identify and exclude the micrograph captions, then the deep learning algorithm was applied to identify a region of interest (ROI) surrounding the GBM. Next, images were manually checked for accuracy and any ambiguous or incorrectly labeled areas were excluded. Finally, the deep learning algorithm was again applied, this time with the interface length of the podocyte cell body and the GBM as the measurement output (Fig. 3).

Statistical Analysis: Image analysis measurements were imported from Visiopharm or ImageJ into Excel spreadsheets and calculations were completed in Excel.

Graphs and statistical analyses were completed using GraphPad Prism 7.02 software.

Non-parametric statistics were used to analyze data from this study. Group values were reported as median ± semi-interquartile range (sIQR).

Significant differences between groups were assumed for probability values $p < 0.05$.

An ordinary one-way ANOVA was used to compare treatment groups.

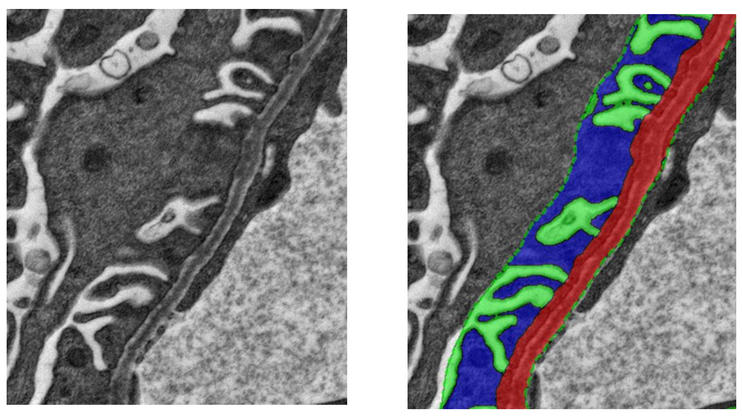

Figure 3
Left – Original Electron micrograph 5000x magnification
Right - Labeled micrograph after image analysis
Blue - Podocytes
Green – Urinary Space
Red – Basement Membrane
Dashed Green – ROI outline

Results

In both the manual and automated measurements of FP width animals induced by injected b\with anti-Fx1a exhibited podocyte foot process effacement versus the sham animals (Fig 4). There was no significant difference between the isotype control group and the groups that received the monoclonal antibodies. The median for the sham groups was nearly identical for both measurement types, however there was much more variation in medians of the groups receiving monoclonal antibodies. The automated measurements had a consistently higher semi interquartile range than the manual measurements.

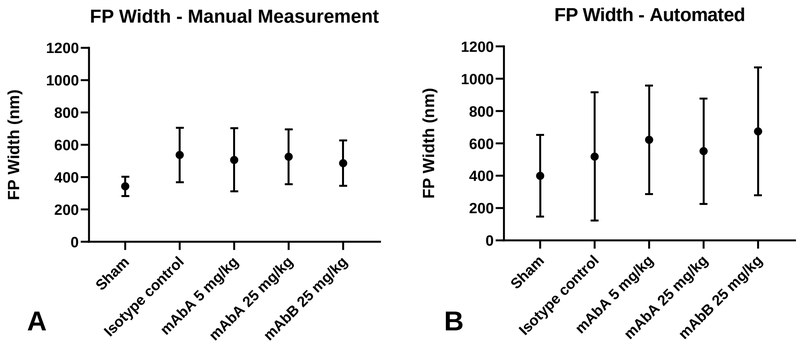

Figure 4
A. Foot Process Width (nm) Measured Manually
B. Foot Process width (nm) Automated Measurement
C. Table of Group Medians and sIQRs

C		Sham	Isotype control	mAbA 5 mg/kg	mAbA 25 mg/kg	mAbB 25 mg/kg
Automated	Median	357.52	409.04	639.61	552.86	692.81
	sIQR	225.57	389.09	247.00	234.53	352.41
Manual	Median	359.30	526.62	464.66	481.19	452.86
	sIQR	46.49	121.30	105.38	131.21	91.59

Discussion

Image analysis protocols were developed to automatically analyze the width of foot processes by measuring the distance between slit diaphragms.

Analysis was limited to a narrow region of interest around the GBM with a ROI defined by a deep learning algorithm. A manual step was required for oversight of the algorithm because since there are no consistent features that deep learning can use to denote which side of the GBM is the lumen versus the urinary space.

In both the manual and automated measurements animals injected with anti-Fx1a exhibited podocyte foot process effacement and a decreased density of slit diaphragms versus the sham animals. There was no significant difference between the isotype control group and the groups that received the test articles.

The automated measurements had a higher median and wider range versus the manual measurements. This is due to the algorithm measuring just above the slit diaphragm rather than the opening itself. A human analyst can easily ascertain the location of the slit diaphragm by taking into account the image context, but the subtle variations in contrast that make up this feature make it difficult to identify even with deep learning. For an approximate solution, the algorithm was designed to measure the FP width just above the slit diaphragms where the FPs began to come apart and have the lighter areas of urinary space between them (Fig. 3)

Deep learning was used to reduce the time spent manually annotating and measuring morphological changes in electron micrographs. In this case AI did not eliminate all manual steps but it did greatly reduce the time spent analyzing images. Further improvement could be achieved with more careful TEM preparation and imaging. The micrographs analyzed in this study were initially taken with manual measurement as the intended endpoint, however if they had been acquired with automated analysis as the endpoint the analysis may have required less stringently quality control and thus reduced analysis time. Additionally, the very nature of manual versus deep learning-based measurements expose biases in each method. Even though the images were blinded, the morphological differences between sham animals and those that received the Anti-FX1A are easily distinguished which could lead to unintentional bias in manual measurement. For the deep learning method, areas were excluded when they were inaccurately classified. This creates a selection bias for less dense areas since the dense areas were prone to inaccurate classification and therefore excluded from the automated measurement.

The images analyzed in this study were optimized for manual measurement. Images were obtained with an aesthetic for composition that preserved the context of the FPs and GBM within the loop and composed to include as much GBM length as possible and an informational caption with scale was included. Since a human can “read through” artifacts, knife marks from sectioning, dirt, and holes in the section were not avoided unless severe.

These selection criteria present challenges to the deep learning algorithm. Adjustments to selection criteria would improve AI accuracy and further reduce the need for manual oversight. Artifacts can affect the distribution of contrast in an image as well as confound the algorithm and should be avoided. Additionally, context, aesthetics and captions are of no use to a deep learning algorithm. Images that are free of any sort of compression due to fixation, sampling or sectioning are most accurately classified.

In addition to refining the image selection criteria future directions of interest include automatic detection and measurement GBM thickness and dense deposit size and frequency. Images in this study were captured in 8-bit greyscale but 16-bit greyscale images may provide a better analysis substrate due to the wider range of intensities. Capturing images without automatically adjusted contrast may also aid the algorithm in accurate classification.

References

Mundel P, Shankland SJ. Podocyte biology and response to injury. Journal of the American Society of Nephrology, 13 (2002), pp. 3005-3015

Kriz W, Shirato I, Nagata M, LeHir M, Lemley KV. The podocyte's response to stress: the enigma of foot process effacement. American Journal of Physiology, Renal Physiology, 304 (2013), pp. F333-F347

Ichinose K, Kitamura M, Sato S, Fujikawa K, Horai Y, Matsuoka N, Tsuboi M, Nonaka F, Shimizu T, Fukui S, Umeda M, Koga T, Kawashiri SY, Iwamoto N, Igawa T, Tamai M, Nakamura H, Origuchi T, Nishino T, Kawakami A. Podocyte foot process width is a prediction marker for complete renal response at 6 and 12 months after induction therapy in lupus nephritis. Clin Immunol. 2018 Dec;197:161-168.

Breakthroughs that change patients’ lives

All procedures performed on animals were in accordance with regulations and established guidelines and were reviewed and approved by Pfizer’s Institutional Animal Care and Use Committee.

Pfizer WORLDWIDE RESEARCH, DEVELOPMENT AND MEDICAL